Optics & Laser Technology 45 (2013) 756–762

Contents lists available at SciVerse ScienceDirect

Optics & Laser Technology

journal homepage: www.elsevier.com/locate/optlastec

Edge and corner detection by color invariants

Jun Chu [a], Jun Miao [b,c,*], Guimei Zhang [c], Lu Wang [a]

[a] School of Software, Nanchang Hangkong University, Nanchang 330063, China
[b] School of Mechatronics Engineering, Nanchang University, Nanchang 330031, China
[c] School of Aeronautical Mechanical Engineering, Nanchang Hangkong University, Nanchang 330063, China

ARTICLE INFO

Article history:
Received 23 February 2012
Received in revised form
12 April 2012
Accepted 27 April 2012
Available online 24 May 2012

Keywords:
Image segmentation
Feature detection
Color invariant

ABSTRACT

Gray-based features are widely used in computer vision applications, while image color is a very important source, which can provide more feature information. To fully exploit color data, a color saturation invariant based on dichromatic reflection model is first constructed. The invariant is an object reflectance property independent of viewpoint and illumination direction. The saturation invariant is then synthesized with existing hue invariant to detect edge and corner features in color image. Experiments show that the detection method proposed here can more effectively tap into color information and achieve true target features due to its lower sensitivity to shadow, shading and highlight. Moreover, when comparing with many other existing edges and corners detecting methods, experimental results demonstrate that the proposed method performs better in detection accurate and effective.

1. Introduction

Detection of low-dimensional features (edges, corners etc.) plays an important role in computer vision applications, such as image segmentation, 3D reconstruction, object recognition etc. [1–3]. Although the majority of images we collect currently are color images, current methods of detecting features only exploit gray information, such as Canny [4], Harris [5], Sift and so on. Sift was proved in [6] to be one of the best features detection and features description algorithms. But it is only designed for gray images instead of color images. When color image features are detected by using gray information, it is hard to distinguish between shadow/highlight and real object.

Compare to gray images, color images provide more diverse information, so features detection based on color images becomes increasingly striking. Burghouts [7] et al. compared the discriminability between gray and color invariants of images. Their experiments show that the extension of gray invariant to color space can enhance discriminability of invariants. For example, integration of color information into Sift descriptor largely improves its performance. Hence, color invariants will be widely applicable in numerous computer vision fields. Montesinos [8] proposed an extension of the luminance Harris corner detector to RGB color model, and recomputed local auto-correlation matrix for corner detection. The approach also results in error detection due to quite strong correlations among three channels. Sebe [9] integrated image's colors into Harris corner detection. They transformed common photometric invariants to the opponent color space and m-color space, and make a judge of feature points by image derivatives. Their work shows that color information can make a significant contribution to feature detection and matching.

A step forward in developing the color invariant was made by Weijer [10], who defined photometric quasi-invariants used in Harris detection for edges and corners in color images. But since reflectance spectrum changes with light source shining upon varied objects, colors in images change also and have a large impact on the detection results, including numerous noise points and wrongly detected edges. In the following work, Weijer [11] made statistics of color derivatives of over 40,000 images in Corel image library, and replaced gray information entropy with color information entropy, so as to implant distinctness information on color in feature detector. But in consideration that each color component in RGB color space is auto-correlative, such an approach still fails to detect true figures of such regions as shadow, highlight etc.

Most segmentation techniques for color images are an extension of grayed-method by transforming R, G and B in linear or non-linear way. Those methods are more useful when computing geometrical variations such as translation, rotation, scale variation and affine transformation, but meet huge challenges in eliminating interference generated by photometric variations such as illumination direction, shadow, shading, and highlight. Geusebroke [12] derived a kind of dichromatic reflection model for reflection of object on lighting according from traditional

* Corresponding author at: School of Software, Nanchang Hangkong University, Nanchang 330063, China.
E-mail addresses: chujun99602@163.com (J. Chu), miaojun0401@163.com (J. Miao), GuimeiZhang@nchu.edu.cn (G. Zhang), LuWang@nchu.edu.cn (L. Wang).

0030-3992/$ - see front matter © 2012 Elsevier Ltd. All rights reserved.
http://dx.doi.org/10.1016/j.optlastec.2012.04.040

Kubelka-Munk theory, thus established a framework of measurement of objective reflectivity and developed a series of color invariants by building connection between reflection model and image difference characteristics. Abdel-Hakim [13] extended Sift descriptors to color scale space, based on the invariants developed by Geusebroke and presented a color Sift (CSIFT). He detected the interest points at the extreme of a difference of Gaussian pyramid in the color space of the input image, and acquired more stabilized colored feature points. But with the method only confined to hue information of images and saturation information is ignored, features within similar hue areas are easily lost when similar hue is available in image.

In this paper, we are primarily concerned with the color information of an image used to detect the correct and robust features, which possess lower sensitivity to photometric variations. In order to resolve the problems in feature detection within similar hue areas, the paper suggests a color saturation invariant with equal energy in uniform illuminance, which is based on framework of measurement of objective reflectivity in colored image supposed by Geusebroke. We then combine such an invariant to hue invariants as proposed by Geusebroke to detect edges and corners. Experiments results show that our method is more adequate for color image detection than 1D hue invariant, while still retaining the ability of discounting scene identical events.

2. Background and related work

2.1. Dichromatic reflection model

Dichromatic reflection model commonly used for color mode analyses the reflected spectra of color bodies based on the old Kubelka-Munk theory. Under the assumption that the material is neither transparent nor translucent, with internal light isotropically scattered. The reflection of the light consists of two parts: the body reflection part and the interface reflection part. The body reflection shows the light which is reflected after penetrating in the surface, while the interface reflection part shows the light which is reflected on the surface immediately. Hence, the color image of an object can be considered as a response which is composed of different primary color sensors. The response is formulated as:

$$E(\lambda,\vec{x}) = m_b(\vec{x})c_b(\lambda,\vec{x}) + m_i(\vec{x})c_i(\lambda,\vec{x}) \tag{1}$$

Where λ is the wavelength and $\vec{x}$ is 2D vector which denotes the image position. $c_b(\lambda,\vec{x})$ denotes the color of the body reflectance and $c_i(\lambda,\vec{x})$ is the color of interface reflectance. m_b and m_i represent the body reflection and surface reflection respectively.

In Eq. (1), $m_b(\vec{x}) = (1-\rho_f(\vec{x}))^2, m_i(\vec{x}) = \rho_f(\vec{x}), c_b(\lambda,\vec{x}) = e(\lambda,\vec{x})R_\infty(\lambda,\vec{x})$ and $c_i(\lambda,\vec{x}) = e(\lambda,\vec{x})$.

Therefore, Eq. (1) can be rewritten as follows:

$$E(\lambda,\vec{x}) = e(\lambda,\vec{x})(1-\rho_f(\vec{x}))^2 R_\infty(\lambda,\vec{x}) + e(\lambda,\vec{x})\rho_f(\vec{x}) \tag{2}$$

In which, $e(\lambda,\vec{x})$ denotes the illumination spectrum, $\rho_f(\vec{x})$ is the Fresnel reflectance at $\vec{x}$ and $R_\infty(\lambda,\vec{x})$ is the material reflectivity. The reflected spectrum in the viewing direction is given by $E(\lambda,\vec{x})$.

For an equal energy illumination, the spectral components of the source are constant over the wavelengths and variable over the position. So a spatial component $i(x)$ denotes intensity variations, resulting in.

$$E(\lambda,\vec{x}) = i(x)(1-\rho_f(\vec{x}))^2 R_\infty(\lambda,\vec{x}) + i(x)\rho_f(\vec{x}) \tag{3}$$

Note that from Eq. (1) the reflected spectrum is divided into two parts by the dichromatic reflection model: a body reflection part which describes the real features of an object and the interface reflection part which contains features of shadow, specular and shade on the image.

2.2. The color invariant related to Hue

In this section, a brief description of the hue invariant developed by Geusebroek [12] is first given.

By Taylor expansion with respect to λ_0, will be.

$$E(\lambda_0+\Delta\lambda) \approx E(\lambda_0) + \Delta\lambda E_\lambda(\lambda_0) + \frac{1}{2}\Delta\lambda^2 E_{\lambda\lambda}(\lambda_0) \tag{4}$$

By differentiating Eq. (3) with respect to λ, giving.

$$E_\lambda = i(x)(1-\rho_f(\vec{x}))^2 \frac{\partial R_\infty(\lambda,\vec{x})}{\partial\lambda} \tag{5}$$

$$E_{\lambda\lambda} = i(x)(1-\rho_f(\vec{x}))^2 \frac{\partial^2 R_\infty(\lambda,\vec{x})}{\partial\lambda^2} \tag{6}$$

By dividing Eq. (5) by Eq. (6) gives.

$$H = \frac{E_\lambda}{E_{\lambda\lambda}} = \frac{\partial R_\infty(\lambda,\vec{x})}{\partial\lambda} \Big/ \frac{\partial^2 R_\infty(\lambda,\vec{x})}{\partial\lambda^2} = f(R_\infty(\lambda,\vec{x})) \tag{7}$$

Geusebroek [12] proved that H is a hue invariant of color. It is an object reflectance property independent of viewpoint, surface orientation, illumination direction, light intensity and Fresnel reflectance coefficient. As the second order spectral derivative vanishes, H is ill-defined. Therefore, the arctan(H), a monotonic function, is substituted for calculating differentiation of H with respect to λ or $\vec{x}$. For example, differential of arctan(H) with respect to $\vec{x}$ results in.

$$H_{\vec{x}} = \frac{\partial(\arctan(H))}{\partial\vec{x}} = \frac{E_{\lambda\vec{x}}E_{\lambda\lambda} - E_\lambda E_{\lambda\lambda\vec{x}}}{E_\lambda^2 + E_{\lambda\lambda}^2} \tag{8}$$

3. The invarianct relating to saturation and features detection

Since the invariant is based purely on the hue information, some material features can be easily missing in similar hue regions while conducting features detection. Saturation is the description of a color relative to its own brightness. Hue and saturation invariants are both needed for human vision to differ chromatic from achromatic information in order to distinguish different states of an object. Therefore, in this section, our aim is to propose an invariant related to saturation and then incorporate it to hue invariant to detect edges and corners in color images.

3.1. Dichromatic reflection model

Under the assumptions that the material is neither transparent nor translucent, and light within the material is isotropically scattered and constant in energy density, dividing (3) by (5) results in.

$$\frac{E(\lambda)}{E_\lambda} = i(x)\frac{(1-\rho_f(\vec{x}))^2 R_\infty(\lambda,\vec{x}) + i(x)\rho_f(\vec{x})}{i(x)(1-\rho_f(\vec{x}))^2[\partial R_\infty(\lambda,\vec{x})]/\partial\lambda}$$
$$= \frac{R_\infty(\lambda,\vec{x})}{[\partial R_\infty(\lambda,\vec{x})]/\partial\lambda} + \frac{\rho_f(\vec{x})}{(1-\rho_f(\vec{x}))^2}\frac{1}{[\partial R_\infty(\lambda,\vec{x})]/\partial\lambda} \tag{9}$$

By considering uniform surfaces, a single and uniform illumination within the dichromatic reflection model, the material reflectivity R_∞ and Fresnel reflectance ρ_f are both independent of $\vec{x}$.

$$\frac{E(\lambda)}{E_\lambda} = \frac{R_\infty(\lambda)}{(\partial R_\infty(\lambda))/\partial\lambda} + \frac{\rho_f}{(1-\rho_f)^2}\frac{1}{(\partial R_\infty(\lambda))/\partial\lambda} \tag{10}$$

It is noted that $E(\lambda)/E_\lambda$ depends on the energy of incident light. If some light with certain wavelength accounts for a larger proportion in color information of an image, the corresponding color saturation of the wavelength will be greater. Therefore, $E(\lambda)/E_\lambda$ relates to the saturation of the color. When considering $E/E_{\lambda\lambda}$, the same conclusion could be reached. The properties $E_{\lambda x}$ and $E_{\lambda\lambda x}$ may be interpreted as the intensity normalized spatial derivatives of spectral slope E_λ and spectral curvature $E_{\lambda\lambda}$ respectively. Hence, an invariance related to saturation of the color is given by

$$S=\sqrt{\left(\frac{E}{E_\lambda}\right)^2+\left(\frac{E}{E_{\lambda\lambda}}\right)^2} \tag{11}$$

The data of the color image is acquired from RGB color space. However, the spectra differential coefficient $(E,E_\lambda,E_{\lambda\lambda})$ is derived from the physical model for objects in response to incident illumination. In order to establish a connection between these invariants and the known RGB color space, the Gaussian color model [14] can be used as a general model to measure the spectral information. A linear transformation is used to obtain spectral differential quotients $(\hat{E},\hat{E}_\lambda,\hat{E}_{\lambda\lambda})$ from the RGB values to the Gaussian color model.

$$\begin{bmatrix}\hat{E}\\ \hat{E}_\lambda\\ \hat{E}_{\lambda\lambda}\end{bmatrix}=\begin{pmatrix}0.06 & 0.63 & 0.27\\ 0.3 & 0.04 & -0.35\\ 0.34 & -0.6 & 0.17\end{pmatrix}\begin{bmatrix}R\\ G\\ B\end{bmatrix} \tag{12}$$

Where $(\hat{E}_x,\hat{E}_{\lambda x},\hat{E}_{\lambda\lambda x})^T=S_\sigma(E,E_\lambda,E_{\lambda\lambda})^T$.

In which, $S_\sigma()$ denotes Gaussian smooth window.

3.2. Edges detection

Edge detection is a fundamental tool in image processing and computer vision. Most existing edges detectors are only based on discontinuities of image brightness, such as Roberts, Sobel, Prewitt and Canny [5] detectors. Their major problem is the three components of RGB model dependent on each other and associate strongly with intensity. Hence, features detection in gray image is very difficult to discriminate scene incidental events, such as highlights, shadows and shading. While in color image, real edges are much easier to identify. For example, edges between two objects with same brightness but different hues, or two surfaces of the same object with the same hue but different saturations would be found.

Hue is invariant to certain types of highlights, shading, and shadows in the case of in a uniform illumination. Hence, it was considers as 1D color information and used for edge detection in [10,12]. But an edge should be considered as discontinuities in a three-dimensional color space [15]. For example, in Fig. 1(a), we use columns to illustrate the decreasing saturations of a synthesized blue image. Color representation by the hue invariant (H) and the saturation invariant (S) are shown respectively in Fig. 1(b) and (c). Fig. 1(b) shows that, if only hue information is detected, some edges are missing due to the same hue. Besides hue, saturation is also of particular value in the case where the illumination level varies form point to point or image to image. Therefore, in this section, we integrate the saturation invariants (S) with the hue invariants (H) to detect edges.

The steps of our method in edge detection are illustrated in Fig. 2. In step 3, edge strength is computed by using the gradient and direction of the hue and the saturation invariant. The magnitude or edge strength of the gradient and the direction approximates to the result of the formula:

$$G=\sqrt{G_H^2+G_S^2},\theta=\arctan(G_y/G_x) \tag{13}$$

Where,

$$G_H=\sqrt{G_{Hx}^2+G_{Hy}^2},G_S=\sqrt{G_{Sx}^2+G_{Sy}^2},G_x=\sqrt{G_{Hx}^2+G_{Sx}^2},G_y=\sqrt{G_{Hy}^2+G_{Sy}^2}.$$

Where, G_x denotes the first derivative in the horizontal direction and G_y denotes the first derivative in the vertical direction. G_{Hx} and G_{Hy} denote the first derivative of the hue invariant H in the horizontal and vertical directions. G_{Sx} and G_{Sy} denote the first derivative of the saturation invariant S in the same two directions.

The edge direction angle is rounded to four angles (0, 45, 90, 135 degrees) which respectively representing vertical, horizontal and the two diagonals.

The proposed approach is a generalization of the Canny detector to color data. For other steps in Fig. 2 about the theory please refer to Ref. [4].

3.3. Corners detection

Among intensity gradient based methods, Harris corner detector is the most popular one which identifies corners in an image by using a small Gaussian smooth window which shifts in vertical and horizontal directions along with pixel ordinates. When brightness distribution of a window varies significantly, its center pixel then is defined as corner. Harris corner detector first calculates auto-correlation matrix of gray first order differences, then establishes "corner figure" by calculating corner measure for each pixel to select corner features of image. In this section, we extends Harris detector

Fig. 1. Example of the invariants associated with H and S. (a) A synthesized blue image with the decreasing saturations. (b) The hue distribution of (a). (c) The saturation distribution of (a). The S shows the purity at color borders. (For interpretation of the references to color in this figure legend, the reader is referred to the web version of this article.)

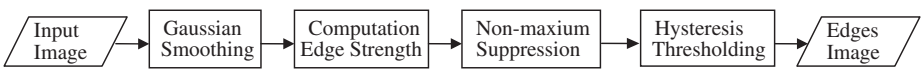

Fig. 2. Flow diagram of edge detection.

in color space, present a method of detecting corners in color images with the invariants related to hue and saturation. For color images, gray differences in Harris detector are replaced with first order differences relevant to hue and saturation invariants to calculate auto-correlation matrix M of each pixel in image.

$$M=\begin{bmatrix} M_{11} & M_{12} \\ M_{21} & M_{22} \end{bmatrix} \tag{14}$$

Where $M_{11}=S_\sigma(H_x^2+S_x^2), M_{22}=S_\sigma(H_y^2+S_y^2), M_{12}=M_{21}=S_\sigma(H_xH_y+S_xS_y), S_\sigma()$ stands for a Gaussian smoothing window. H_x and H_y denote the color gradient value of image ordinates in vertical and horizontal directions. S_x and S_y stand for saturation gradient value of image ordinates in vertical and horizontal directions.

$$H_x=\frac{\partial(\arctan(H))}{\partial x}=\frac{E_{\lambda x}E_{\lambda\lambda}-E_\lambda E_{\lambda\lambda x}}{E_\lambda^2+E_{\lambda\lambda}^2},$$

$$H_y=\frac{\partial(\arctan(H))}{\partial y}=\frac{E_{\lambda y}E_{\lambda\lambda}-E_\lambda E_{\lambda\lambda y}}{E_\lambda^2+E_{\lambda\lambda}^2},$$

$$S_x=\frac{\partial(\arctan(S))}{\partial x}=\frac{E_x(E_\lambda^2+E_{\lambda\lambda}^2)-E(E_\lambda E_{\lambda x}+E_{\lambda\lambda}E_{\lambda\lambda x})}{(E_\lambda^2+E_{\lambda\lambda}^2+E^2)\sqrt{E_\lambda^2+E_{\lambda\lambda}^2}},$$

$$S_y=\frac{\partial(\arctan(S))}{\partial y}=\frac{E_y(E_\lambda^2+E_{\lambda\lambda}^2)-E(E_\lambda E_{\lambda y}+E_{\lambda\lambda}E_{\lambda\lambda y})}{(E_\lambda^2+E_{\lambda\lambda}^2+E^2)\sqrt{E_\lambda^2+E_{\lambda\lambda}^2}}.$$

Then, the strength of interest points is measured by the computation of $I(x,y)$.

$$I(x,y)=Det(M)-k[Trace(M)]^2 \tag{15}$$

Where $Det(M)=M_{11}M_{22}-M_{12}M_{21}$, $Trace(M)=M_{11}+M_{22}$.

To eliminate contour points with one strong eigenvalue, the second term k is set as 0.04. A 3×3 mask is used to make non-maximum suppression which is applied in the interest point strength. Finally, a threshold is used to select interest points. The threshold is set to be changeable to get the amount of corners we specify.

4. Experimental results

4.1. Edges detection Experiments

To evaluate the proposed approach, experiments are performed on more than 300 color images collected from Google Image. First, an example is demonstrated in Fig. 3 to show the potential of a saturation invariant proposed by us on edge detection. In order to make a separate evaluation on contribution of the saturation invariant, we suppose $G_s=0$ in Eq. (13) for the purpose that only hue part is left in Eq. (13). In this way, edge detection method given in last section is actually a calculation by replacing luminance in gray image with hue. Fig. 3(c) shows that edges of most object material can be detected successfully, but edges become vague on the surfaces with similar hue. For instance, in Fig. 3(a) (image to be detected), seamed edges of the cubes in the upper and lower left corner are not found. When G_H is set as 0, only saturation item is left in the equation. The result is shown in Fig. 3(d). Note that the missing edges of two cubes are detected successfully. But Fig. 3(d) also indicates edges of object in the lower right corner in Fig. 3(c), which should have been detected successfully, but failed. Fig. 3(e) demonstrates the results of combining hue invariant with saturation invariant, and note that such results can be considered as complementary results between Fig. 3(c) and (d). Also, the results above indicate our method not only makes a full use of hue and saturation information, but also rules out instable results in coincident part of information. Fig. 3(b) shows detection results by the invariants of normalized RGB [10] which lead to misleading detection results due to impacts of scene incidental events (highlight and shadow, etc).

In Fig. 4, we compare the edge detection results of our method with the hue invariant method and two other commonly used methods: luminance canny detector [4] and the normalized RGB detector [10]. Edges position is determined by a hysteresis threshold. Fig. 4(a) is input image. Note that, in Fig. 4(b), luminance canny detector is most sensitive to influence of scene incidental events. Nevertheless, as shown in Fig. 4(c), the normalized RGB detector doesn't fare any better because of the close relation of the three components of RGB color system. The hue invariant known as a shadow, shading and specular invariant has a strong resistance to scene incident events. But as shown in Fig. 4(d), it missed some edges due to only using hue information in image. The result of our method is successful as shown in Fig. 4(e) in discounting scene incidental events and detecting most object edges (material edges). However, in order to calculate the second derivative, our algorithm needs more computation. A quantitative comparison of their responses to edge derivatives is shown in Fig. 4(f). A line indicates the location of response is depicted in Fig. 4(a). It crosses the object edges and several shading and specular edges. In Fig. 4(f), for convenience of comparing these methods, the derivatives strength is normalized in the domain from 0 to 1. The horizontal ordinate denotes the image position. It clearly shows that our method has the most obvious gap and almost perfectly runs through the non-object edges. However, luminance canny detector is quite opposite. There is severe disturbance in the non-object boundary area, so most edges detected are not real.

4.2. Corners detection Experiments

In order to evaluate algorithm objectively, we use a large number of color images in different imaging conditions including illumination directions, illumination intensities and object viewpoints. For the purpose of evaluation, we compare the performance of our method with that of the other four corner detectors: Luminance Harris (LHarris) [5], Color Harris (CHarris) [8], Color Boosting Harris (CBHarris) [11] and corner detector based on specula shadow-shading quasi invariant(SSSQICorner) [10]. We compare those corner detectors according to two criteria: ground-truth verification and repeatability.

1) *Experiments for Ground-truth Verification*: Ground-truth verification is a commonly used evaluation method, but it can only

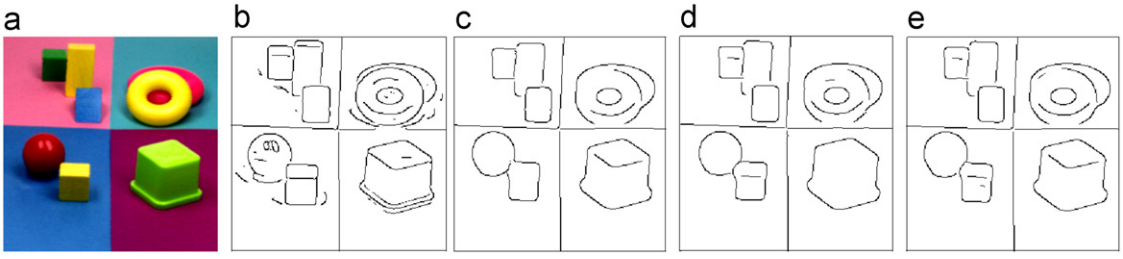

Fig. 3. (a) Input image. Edge detection results based on (b) the normalized RGB, (c) the hue invariant (H), (d) the saturation invariant (S) and (e) the proposed method.

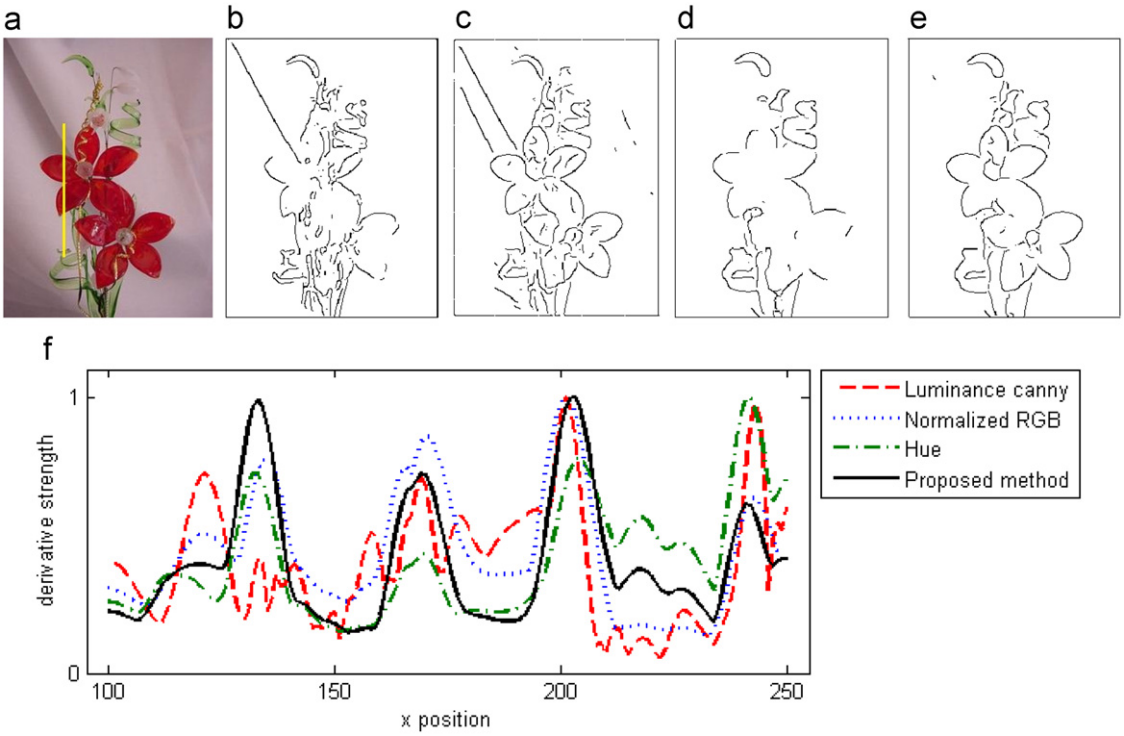

Fig. 4. (a) Input image with a superimposed yellow line which are plotted in the image (f). Edge detection based on (b) luminance canny detector, (c) the normalized RGB, (d) hue invariant (H), (e) the proposed method. (f) The derivative strength along the line indicated in (a).

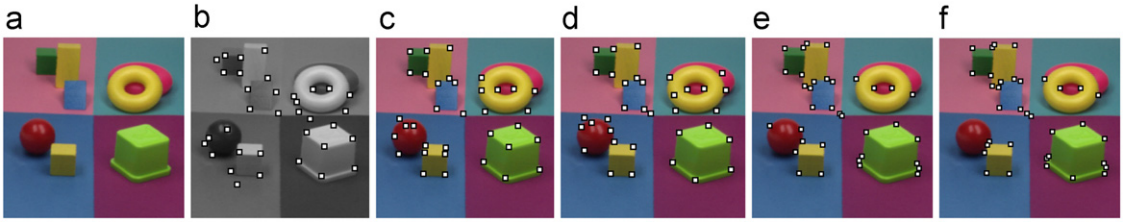

Fig. 5. (a) Input image. Results of corner detection based on (b) LHarris, (c) CHarris, (d) CBHarris, (e) SSSQICorner, (f) Proposed detector, image in (e) and (f) ignore the shadow, the shading and the specular corners.

identify obvious corners in the image, yet facing difficulty in deciding whether a point should be classified as a corner or not. In order to evaluate the performance of detectors more authentically, we use a uniform parameter for the general purpose of feature detection. In Fig. 5, Corners appear in the areas where changes in color and illumination occur. Fig. 5 shows the most prominent 35 corners detected by the five methods above. Note that all detectors can detect most of corners in images. However, since the three primary colors of the RGB mode are interconnected, Lharris (Fig. 5(b)), Charris (Fig. 5(c)) and CBHarris (Fig. 5(d)) are difficult to resist the influence of specular corners and shadows (around the red ball). Our method (Fig. 5(f)) shows better performance by calculating the hue information, as well as SSSQICorner (Fig. 5(e)).

Table 1 demonstrates a test of the corner detection accuracy of the invariant with respect to photometric changes. The experiment is performed with detecting corners of a specific object and is executed on the set of images ALOI 450_png4 listed in http://staff.science.uva.nl/~aloi/, which comprises of 12 images with different illumination spectra and 8 images (Camera 1 set) with different illumination directions (see Figs. 6 and 7). For each image and invariant, the 50 most prominent corners are detected. The derivatives are computed with a Gaussian derivative of $\sigma=1.5$. As the luminance axis remains the major axis of variation in the RGB-cube, the results of the first three methods have been greatly affected. LHarris resulting in the most instable corners is the worst. Neither CHarris (c) nor CBHarris makes greater progress yet. Meanwhile, using color invariants instead of gray value in the last two methods guarantees the ground-truth with respect to photometric changes. Results show that SSSQICorner and the proposed detector outperform the others.

Table 1
Percentage of falsely detected corners.

	Detection error %	
	Changes in illumination spectra	Changes in illumination direction
LHarris	23.5	52.3
CHarris	22.1	51
CBHarris	22.3	50.2
SSSQICorner	1.3	23
Proposed detector	3.9	11.8

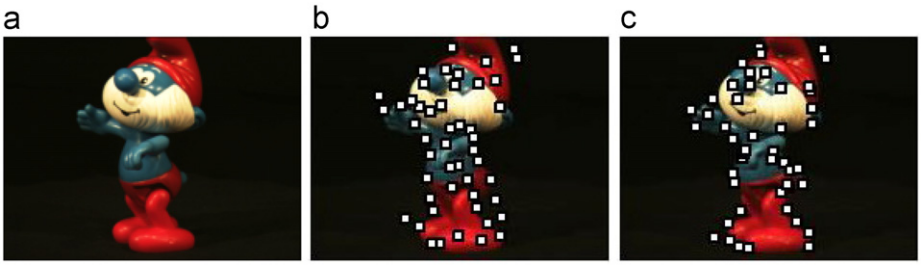

Fig. 6. (a) An example from ALOI 450_png4 image with 2175 K illumination color temperature and the corner detecting results based on (b) SSSQICorner, and (c) the proposed detector.

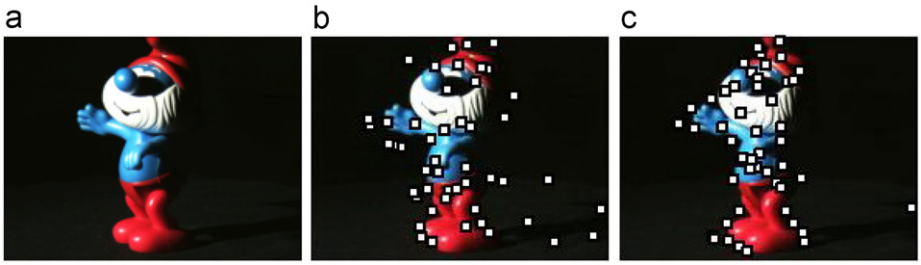

Fig. 7. (a) An example from ALOI 450_png4 image under a particular illumination direction and corner detecting results based on (b) SSSQICorner, and (c) the proposed detector.

Fig. 8. Results of corner detector based on CBHarris (Top) and the proposed detector (Bottom). At first glance, the proposed detector has a better stability.

Furthermore, we make a comparison as shown in Fig. 8 between SSSQICorner and our method. Note that the images have several discrete areas, including specular area (the sky) and darkness area (the tree). It is clear that the tower is the main target in the image. As the number of the detected corners increases, the corners of SSSQICorner (top) appear increasingly in both specular area and darkness area. However, our method results in a more stable performance and corners are dominant on the main target (the tower). Moreover, although the total number of detected corners depends on thresholding constraints, it is noted at first glance that our method has a better repeatability than SSSQICorner.

2) *Experiments for Repeatability*: Repeatability signifies detection is independent of changes in the imaging conditions. This indicates how many detected corners are repeated in both images. As described in [16], the repeatability rate r_i for image I_i is defined by

$$r_i = \frac{R_i}{\min(n_1, n_i)} \tag{16}$$

where R_i is the number of point-to-point correspondences. n_1 and n_i are corners detected in the common part of images I_1 and I_i. Fig. 9 (top) shows the detected images of a sample object in different illumination directions, intensities and color light

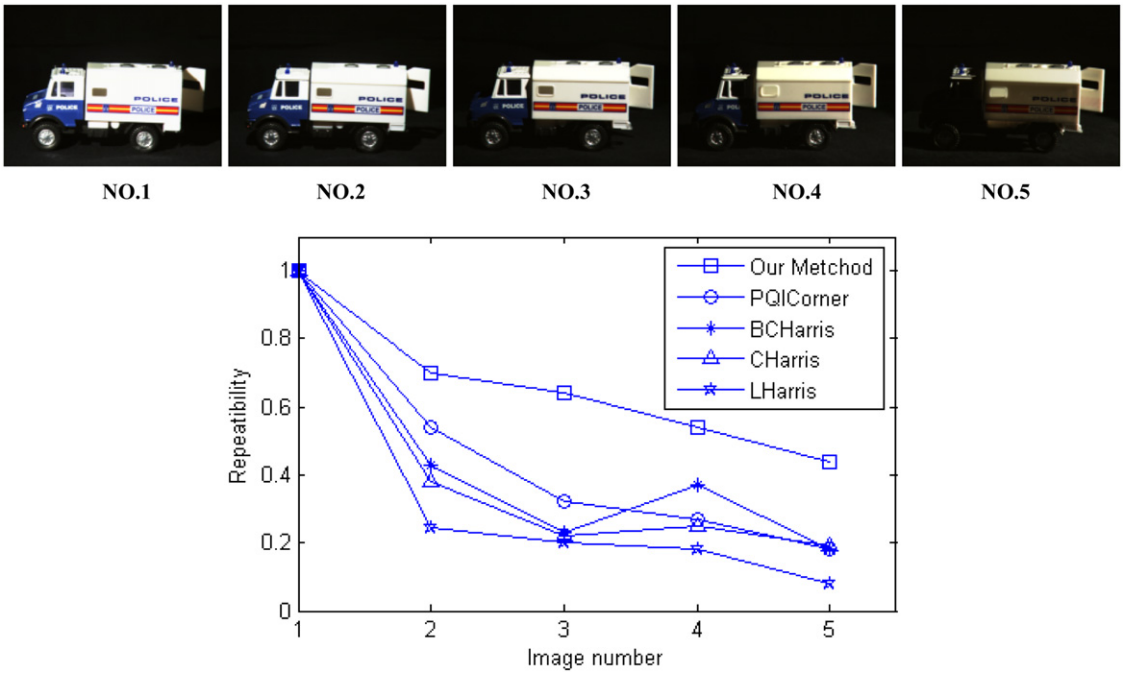

Fig. 9. Images of one test sequence for repeatability is shown at top, while the bottom graph displays repeatability of detectors.

sources. Results show that LHarris, CHarris and CBHarris have a worse repeatability. SSSQICorner does not give a better result either due to light source changes. Our method gives a much better result than the other detectors thanks to its computation which is based on the hue and the saturation invariance and can be easily adapted to illumination and light source changes.

5. Conclusion

Based on the dichromatic reflection model which mirrors object surface′s reflection of light, the paper presents a saturation invariant in color image, and then integrates it with the hue invariant to detect edges and corners. Experiments show that our method achieves a better performance by using more color information and more effective and stable in terms of body features detection when comparing with many existing methods.

Acknowledgment

This work was supported by the National Natural Science Foundation of China (No. 60954002, 61063030), Aviation Science Foundation of China (No. 2010ZC56005), and Jiangxi Province Education Office Youth Science Fund (No. GJJ10197).

References

[1] Deshmukh KS. Color image segmentation: a review. Proc. of SPIE 2010;7546 754624-1–6.
[2] Laganiere R, Gilbert S, Roth G. Robust object pose estimation from feature-based stereo. IEEE Trans Instrumentation and Measurement 2006;55(4): 1270–80.
[3] Dardas NH, Georganas ND. Real-time hand gesture detection and recognition using bag-of-features and support vector machine techniques. IEEE Trans Instrumentation and Measurement 2011;60(11):3592–607.
[4] Canny J. A computational approach to edge detection. IEEE Trans Pattern Analysis and Machine Intelligence 1986;8(6):679–714.
[5] HarrisC, StephensM. A combined corner and edge detector. In: *Proc. 4th Proc. Alvey Vision Conf.* Manchester, England, 1998; pp. 147–51.
[6] Mikolajczyk K, Schmid C. A performance evaluation of local descriptors. IEEE Trans Pattern Analysis and Machine Intelligence 2005;27(10):1615–30.
[7] Burghouts GJ, Geusebroek JM. Performance evaluation of local colour invariants. In: *Proc. Int. Conf. Computer Vision and Image Understanding*, 2009, vol. 113, no. 1, pp. 48–62.
[8] Montesinos, P, Gouet, V, Deriche R. Differential invariants for color images. In: *Proc. 1998 IEEE Int. Conf. Pattern Recognition*, Queensland, Australia, 1998, pp. 838–40.
[9] Sebe, N, Gevers, T, van de Weijer, J, Dijkstra, S. Corners detectors for affine invariant salient regions: Is color important? In: *Proc. ACM Conf Image and Video Retrieval*, Phoenix, USA, 2006, pp. 61–71.
[10] van de Weijer J, Gevers Th, Geusebroek JM. Edge and crner detection by photometric quasi-invariants. IEEE Trans Pattern Analysis and Machine Intelligence 2005;27(4):625–30.
[11] van de Weijer J, Gevers Th, Bagdanov AD. Boosting Color Saliency in Image Feature Detection. IEEE Trans Pattern Analysis and Machine Intelligence 2006;28(1):150–6.
[12] Geusebroek JM, van den Boomgaard R, Smeulders AWM, Geerts H. Color invariance. IEEE Trans Pattern Analysis and Machine Intelligence 2001;23(12):1338–50.
[13] Abdel-Hakim Alaa E, Farag Aly A. CSIFT: A SIFT Descriptor with Color Invariant Characteristics. In: *Proc. Int. Conf. Comput. Vis. And Pattern Recog.*, New York, USA: 2003, pp. 1978–83.
[14] GeusebroekJan-mark, Van Den BoomgaardRein, SmeuldersArnold WM, DevAnuj. Color and scale: The spatial structure of color images. In: *Proc. Eur. Conf. Comput. Vis.*, 2000, pp. 331–41.
[15] Cheng HD, Jiang XH, Sun Y, Wang Jing Li. Color image segmentation: advances & prospects. Pattern Recognition 2011;34(12):2259–81.
[16] Schmid C, Mohr R, Bauckhage C. Evaluation of interest point detectors. International Journal of Computer Vision 2000;37(2):151–72.